Thermal Science and Engineering Progress 6 (2018) 157–163

Contents lists available at ScienceDirect

Thermal Science and Engineering Progress

journal homepage: www.elsevier.com/locate/tsep

Tempering of water storage tank temperature in hot climates regions using earth water heat exchanger

Salman H. Hammadi

Department of Mechanical Engineering, Engineering College, Basrah University, Iraq

ARTICLE INFO

Keywords:
Cylindrical solar water heater
Cylindrical enclosure
Earth tube heat exchanger

ABSTRACT

In hot climate regions, outdoor domestic water tank is directly exposed to high solar intensity in addition to hot summer wind stream. The storage water temperature increases above 50 °C. In order to overcome this problem, time dependent analysis of cylindrical domestic storage water tank that exposed to high solar radiation is performed. The analysis includes energy balance for the water tank as well as to an earth water heat exchanger used to reduce the water temperature in summer months. The governing equations are solved numerically using fourth order Runge-Kutta method. It is found that using earth water heat exchanger reduces the water temperature by about 16 °C. A comparison of the numerical results with experimental data showed a good agreement.

1. Introduction

Water storage tanks are an essential part of water supply system for residential and commercial buildings. The water tank is placed atop the roof to gravity-feed the buildings. In Iraq summer, the ambient temperature increases above 50 °C due to high solar radiation. As a result, water temperature in the storage tank raised up to 50 °C which makes it inappropriate for domestic use. The local efforts for heat Insulating or solar shading of the water tank have not been efficient. This research is trying to solve this problem via passing the water flowing down from the tank through a heat exchanger buried in the ground at 5 m depth to decrease the water temperature to an acceptable value not exceed 33 °C. The present work is a special case that covered the negative effect of the solar radiation. There are no previous similar studies found in the literatures.

N. M. Nahar and K. S. Malhotra [1] experimentally studied year round performance of 0.05 m^3 cylindrical solar water heater inclined at 40° with horizontal plane. They found that in the summer months, the maximum water temperature is 60 °C when the tap water temperature supplied at 30 °C for the solar radiation 6 kW/m^2 day

S. Saroja et al. [2] studied theoretically and experimentally inclined cylindrical solar water heater. They assumed that the ends of the cylindrical tank are isolated and the curvature effect of the tank is neglected. Unsteady analysis was performed using energy balance equation. They concluded that both the wall and fluid temperature increase with solar heat flux and showed a good agreement between their experimental and theoretical results.

In earth tube heat exchanger field, there are huge numbers of researches deal with cooling or heating of air or water. F. Al-Ajmi et al. [3] presented a theoretical model of an earth air heat exchanger (EAHE) for predicting the outlet air temperature and cooling potential of these devices in a hot, arid climate. Sub-soil temperature model adapted for specific conditions in Kuwait is presented and its output compared with measurements in two locations. The EAHE is shown to have the potential for reducing cooling energy demand in a typical house by 30% over the peak summer season (middle of July). Faezeh Fazlikhani et al. [4] studied numerically the efficiency of earth tube heat exchanger for cold and hot arid climates. The results showed, EAHEs have higher potential to act as cooler in hot-dry climates rather than as a heater in cold climates and the air temperature can be reduced from 40 °C to 24.5 °C for a pipe length of 100 m and soil temperature 18.2 °C at a depth of 14 m.

Sanjeev Jakhar and Manoj S. Soni [5] presented experimental and theoretical analysis for earth water heat exchanger (EWHE) used to cool photovoltaic panels in semi-arid region of Pilani, Rajasthan (India). The results of the experimental study showed that the maximum PV panel temperature goes up to 73 °C without any cooling and the PV panel temperature drops in the range of 43.68–49.64 °C when using EWHE with 38 m length and water flow rate of 0.033 kg/s.

2. Theoretical analysis

The theoretical analysis of the model considered includes PVC water storage tank exposed to solar radiation and earth water heat exchanger buried underground. The following assumptions are made:

E-mail address: slmnhm@yahoo.com.

https://doi.org/10.1016/j.tsep.2018.03.009
Received 26 November 2017; Received in revised form 25 March 2018; Accepted 25 March 2018

Nomenclature

A	area (m^2)
As	annual surface temperature (°C)
C	specific heat (J/kg °C)
D	diameter (m)
F_{ws}	configuration factor of the diffused solar radiation (–)
F_{wG}	configuration factor of the reflected solar radiation (–)
g	acceleration of gravity (m/s^2)
h	heat transfer coefficient (W/m^2 °C)
I	solar radiation (W/m^2)
j	day number from first January
k	thermal conductivity (W/m °C)
L	water storage tank height (m)
L_p	EWHE length (m)
Nu	Nusselt number (–)
Pr	Prandtle number (–)
Ra	Rayleigh number (–)
S	sunshine duration (h)
T	temperature (°C)
t	time (h)
t_l	local time (h)
t_o	phase constant(hr)
U	wind velocity (m/s)
x	horizontal coordinate (m)
z	vertical coordinate (m)

Greek letters

α	soil thermal diffusivity (m/s^2)
φ	latitude angle (degree)
β	compressibility factor (1/K)
ρ	density (kg/m^3)
ϕ	altitude angle (degree)
γ	tilt angle (degree)
δ	declination angle (degree)
ε_g	ground surface reflectivity
θ	incident angle (degree)
ϑ	kinetic viscosity (m/s^2)
τ	hour angle (degree)

Subscript

a	air
DN	direct normal
i	internal
o	external
l	local
p	pipe
s	wall surface
R	reflected
W	water

1. The top and bottom of the water tank is perfectly insulated.
2. Uniform tube wall temperature of EWHE and it is equal to the soil temperature at the given depth.
3. Heat loss from the pipelines is neglected.

2.1. Water storage tank analysis

The energy balance for the tank wall shown in Fig. 1 can be given as:

$$(I_{DN}\cos\theta + I_D + I_R)D_oL - h_a\pi D_oL(T_s - T_a) - h_w\pi D_iL(T_s - T_w) = \rho_s C_s \frac{\pi}{4}(D_o^2 - D_i^2)L\frac{dT_s}{dt} \quad (1)$$

And the energy balance for the water in the tank is [3]:

$$h_w\pi D_iL(T_s - T_w) = \rho_w C_w \frac{\pi}{4}D_i^2 L\frac{dT_w}{dt} \quad (2)$$

For a vertical projected area of the cylindrical tank (D_o L), the solar incident angle (θ) is equal to the altitude angle (ϕ) which is given as follows [6]:

$$\sin\phi = \cos\varphi\cos\tau\cos\delta + \sin\varphi\sin\delta \quad (3)$$

where the hour angle (τ) is given as:

$$\tau = 15(t_l - 12) \quad (4)$$

The heat transfer coefficient from the tank wall to the water can be evaluated using the following free convection relation [7]:

$$Nu_w = 0.046\, Ra^{1/3} \quad (5)$$

where (Ra) is Rayleigh umber which is given by:

$$Ra = \frac{g\ \beta(T_s - T_w)D_i^3 Pr}{\vartheta^2} \quad (6)$$

And

$$\beta = \frac{2}{T_s + T_w} \quad (7)$$

$$h_w = \frac{k_w\ Nu_w}{D_i} \quad (8)$$

The outside heat transfer coefficient is given as [8]:

$$h_a = 5.7 + 3.8U \quad (9)$$

The solar radiation incident on the water tank consists of three components; direct normal solar radiation (I_{DN}), diffused solar radiation (I_D), and reflected solar radiation (I_R). The main component is the direct normal one which can be expressed as a sinewave profile as [9]:

$$I_{DN} = I_{max}\sin\frac{\pi t}{S} \quad (10)$$

where the average experimental values of I_{max} for south of Iraq are tabulated as follows [10] (see Table 1):

And (**S**) is the sunshine duration which can be calculated from the following formula [11]:

$$S = \frac{2}{15}\cos^{-1}[-\tan(\delta)\tan(\varphi)] \quad (11)$$

The declination angle is given as [12]:

$$\delta = 23.45\sin[0.986(j + 284)] \quad (12)$$

The diffused solar radiation for the summer is given as:

$$I_D = 0.135 I_{DN} F_{ws} \quad (13)$$

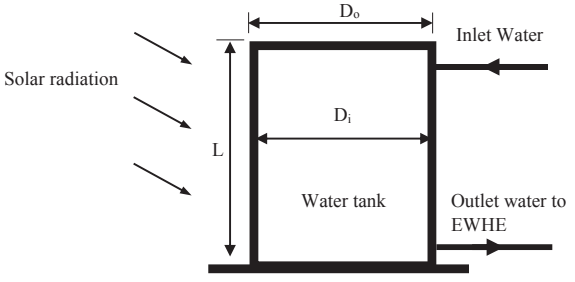

Fig. 1. Cylindrical water storage tank.

Table 1
Experimental maximum direct normal solar radiation [9].

Month	I_{max} (W/m^2)
May	1142
June	1160
July	1178
August	1105

where the configuration factor F_{ws} is [13]:

$$F_{ws} = \frac{1 + \cos\gamma}{2} \tag{14}$$

Also the reflected solar radiation component is calculated as:

$$I_R = [I_{DN} + I_D]\varepsilon_g F_{wG} \tag{15}$$

And

$$F_{wG} = \frac{1-\cos\gamma}{2} \tag{16}$$

Eqs. (1) and (2) are solved simultaneously using equations ((3)–(16)) to evaluate T_s and T_w as a function of time.

3. Earth water heat exchanger

The hot water in the tank flows to earth water heat exchanger buried underground at an arbitrary depth to change its temperature to an acceptable value for residential use. First of all, it's necessary to calculate the soil temperature at any depth and time. The heat conduction equation for the soil can be given as follows [4]:

$$\frac{\partial^2 T}{\partial z^2} = \frac{1}{\alpha}\frac{\partial T}{\partial t} \tag{17}$$

$$\text{At } z = 0 \quad T(0,t) = T_m + A_s\cos\left[\frac{2\pi}{8760}(t-t_o)\right] \tag{18}$$

$$z = \infty \quad T(\infty,t) = T_m$$

The soil temperature can be estimated by solving equation (17) as follows [3]:

$$T(z,t) = T_m - A_s Exp\left[-z\left(\frac{\pi}{8760\ \alpha}\right)^{0.5}\right]\cos\left\{\frac{2\pi}{8760}\left[t-t_o-\frac{z}{2}\left(\frac{8760}{\pi\ \alpha}\right)^{0.5}\right]\right\} \tag{19}$$

Since Basrah city is closed to Kuwait and has similar soil properties and climate conditions, the value of annual mean ground temperature (T_m), annual surface temperature (A_s), soil diffusivity α and phase constant (t_o) are taken as: 27 °C, 13.3 °C, 0.0038 m^2/h and 552 h respectively. So equation (19) becomes [3]:

$$T(z,t) = 27 - 13.3\ Exp(-0.31\ z)\cos\left\{\frac{2\pi}{8760}(t-552-428.31\ z)\right\} \tag{20}$$

The energy balance of earth water heat exchanger shown in the Fig. 2 is:

$$h_p\ \pi\ D_p\ (T_w - T_p)dx = -\dot{m}_w C_w\ dT_w \tag{21}$$

Integrated the above equation with the inlet boundary conditions to the final state as:

$$x = 0,\ T = T_{wi} \tag{22a}$$

$$x = L_p,\ T = T_{wo} \tag{22b}$$

Gives the outlet water temperature for any tube length as:

$$T_{wo} = T_p + (T_w - T_p)\ Exp\left(-h_p\pi\ D_p\frac{L_p}{\dot{m}_w C_w}\right) \tag{23}$$

where T_p is assumed to be equal to the soil temperature $T(z,t)$ at the given depth (z) and time (t).

For laminar inside tube flow of constant wall temperature, the Nusselt number is given as [14]:

$$Nu = 3.66 \tag{24}$$

And the heat transfer coefficient is:

$$h_p = \frac{3.66 k_w}{D_p} \tag{25}$$

The water density and viscosity are given as a temperature dependent as follows:

$$\rho_w = 1001 - 0.08832T_w - 0.00341T_w^2 \tag{26}$$

$$\mu_w = 0.001(1.4 - 0.023T_w + 0.00013T_w^2) \tag{27}$$

4. Results and discussion

The governing time dependent differential equations (1) and (2) are solved simultaneously by fourth order Runge-Kutta method using equations ((3)–(16)) to evaluate the wall temperature (T_s) and water temperature (T_w) as a function of time. In addition, the water temperature outlet from the earth tube heat exchanger (T_{wo}) was evaluated using equation (23). All parameters used in the calculations are given in Table 2

Figs. 3–6 show the tank wall and water temperatures increase with time to reach maximum values at about 17.00 and 18.00 respectively. Its shows that the wall temperature is higher than the water temperature at shine duration and the trend is inflected at night. This is due to the higher mass and specific heat of the water in comparison with the tank wall materials. At night, both the wall and water temperatures decreased due to the heat losses in absent of solar radiation and decreasing of ambient temperature. In all figures, it has observed that, the wall and water temperatures do not return to the initial values at the end of night. This is due to the effect of thermal inertia of PVC and water. It's also noted that the maximum wall and water temperatures for the hotter months (May, June, July, and August) are closed to each other with differences of about (1–2 °C).

Figs. 7–10 explained the behavior of the tank water temperature (T_w) and the water outlet temperature of the earth water heat exchanger (T_{wo}). In all these figures, it is shown that, (T_{wo}) is less fluctuation than (T_w) due to the decrease of the soil temperature fluctuation with the soil depth as shown in the Fig. 12. The water temperature (T_w) is very high and closed to 50 °C in the summer season. This temperature was reduced to acceptable level for residential use by passing the hot water through an earth water heat exchanger to give temperature not exceed 33 °C as shown in Fig. 11 which represents the maximum temperature of the storage water and its corresponding outlet EWHE temperature.

Fig. 13 represents the soil temperature distribution as a function of the soil depth for July (see equation (20)). The soil temperature decreases gradually as the soil depth increases to be ultimately uniform at

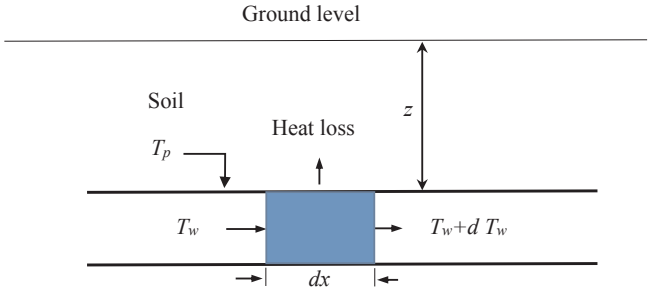

Fig. 2. Energy balance of the earth water heat exchanger.

Table 2
Values of the model parameters.

Parameter	Numerical Value
Water tank outside diameter	1.15 m
Water tank inside diameter	1.12 m
Water tank height	1 m
PVC density	1350 kg/m^3
PVC specific heat	1200 kJ/kg °C
Water specific heat	4.19 kJ/kg °C
Water thermal conductivity	0.6 W/m °C
Diameter of EWHE tube	10 cm
Air velocity	4 m/s
EWHE water mass flow rate	0.05 kg/s
Ground surface reflectivity	0.6

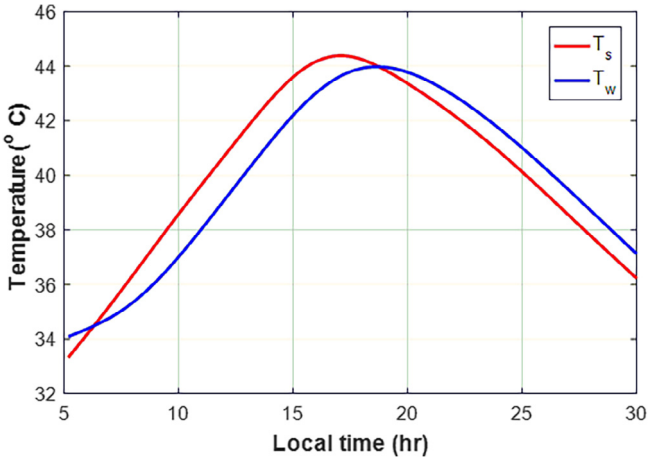

Fig. 3. Daily water and tank temperature profiles (May).

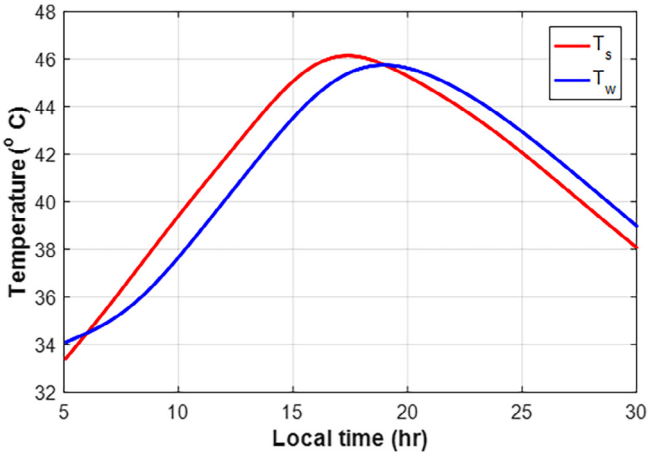

Fig. 4. Daily water and tank temperature profiles (June).

a depth of about 8 m.

Fig. 14 showed the EWHE outlet water temperature with its length for selected two summer months (June and August). In general, the temperature decreases with the tube length due to the increase of heat transfer area between the water and soil. August water temperature is higher than that of June due to the higher soil temperature in August because of accumulated solar heating of the soil as shown in Fig. 12.

4.1. Model validation

Field-testing data was used to verify the theoretical model. An existing roof tank test of 1 m^3 volume shown in Fig. 15 is located in Basra in the south of Iraq. The experimental data was recorded for a selected

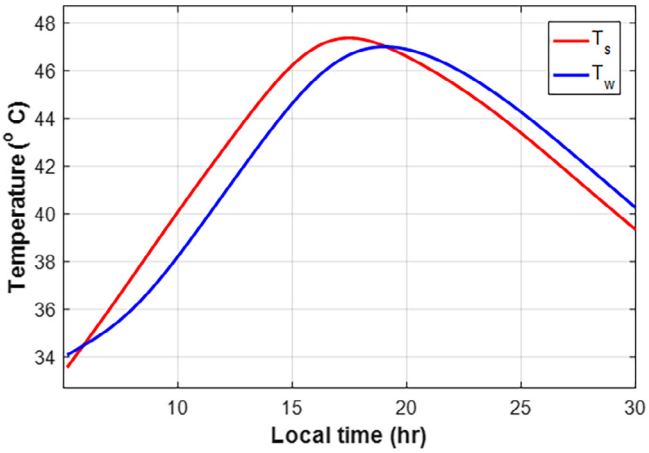

Fig. 5. Daily water and tank temperature profiles (July).

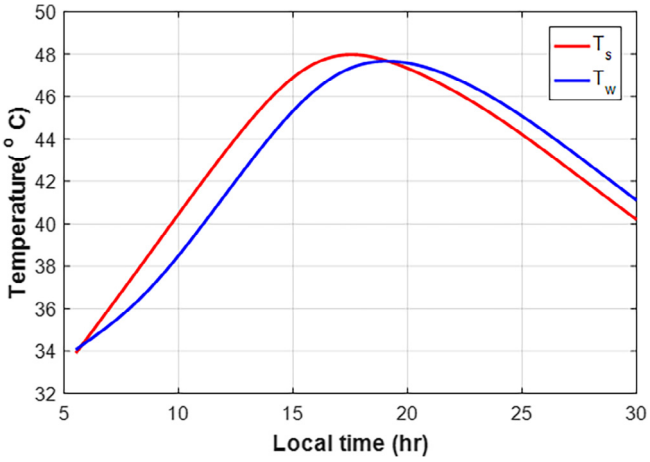

Fig. 6. Daily water and tank temperature profiles (August).

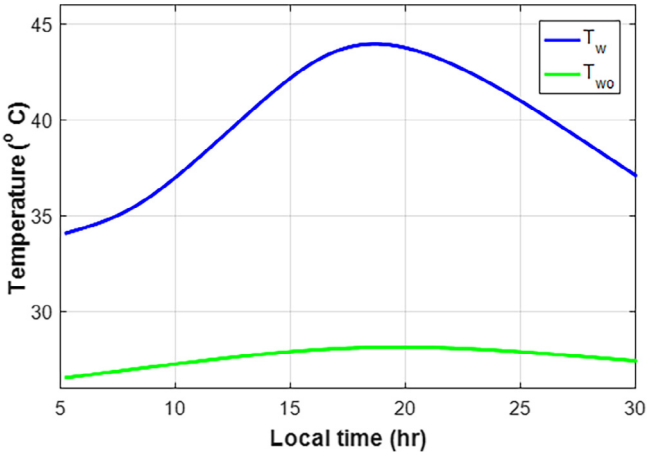

Fig. 7. Daily temperature profile of tank water and outlet water of EWHE (May).

day (25/8/2017). Hourly water temperatures were measured at four points with different depths inside the tank. Average of the water temperature range was adopted in the validation curve shown in Fig. 16.

4.1.1. Error analysis

The error calculation for the recorded water temperatures can be given as follows [15]:

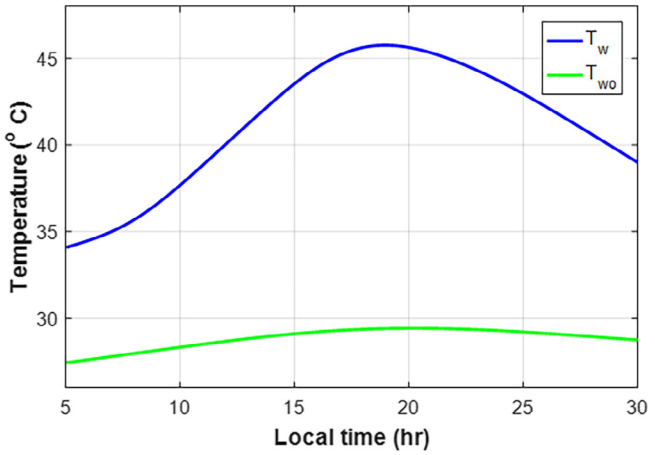

Fig. 8. Daily temperature profile of tank water and outlet water of EWHE (June).

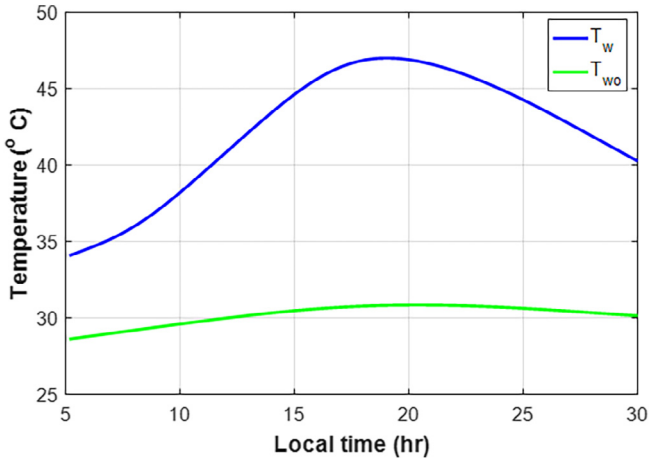

Fig. 9. Daily temperature profile of tank water and outlet water of EWHE (July).

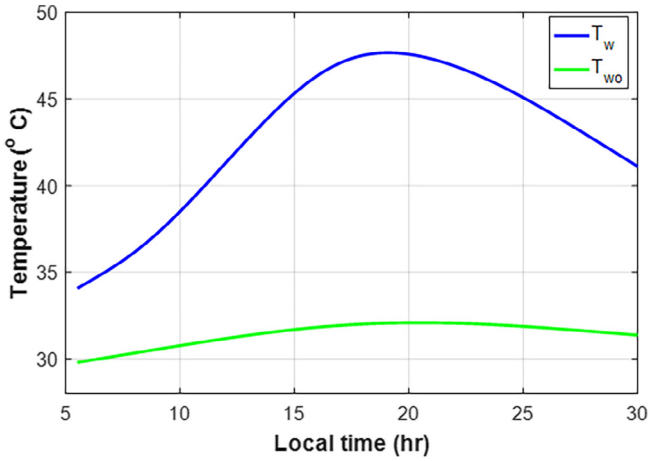

Fig. 10. Daily temperature profile of tank water and outlet water of EWHE (August).

$$SD = \sqrt{\frac{(T_w - Tw_{av})^2}{n-1}} \tag{28}$$

And;

$$SE = \frac{SD}{\sqrt{n}} \tag{29}$$

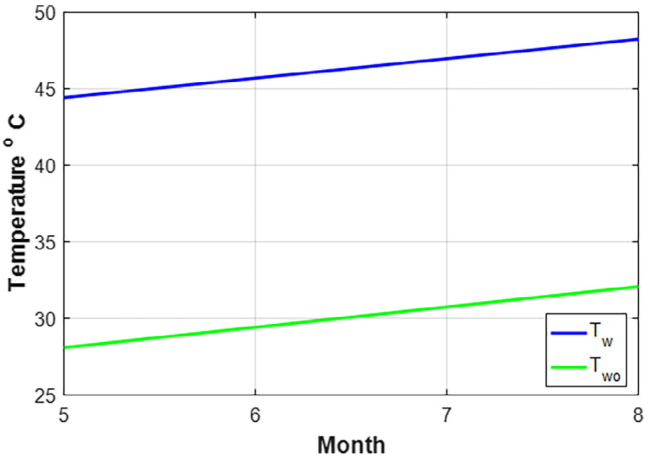

Fig. 11. Monthly water temperature profiles of the storage tank and water at outlet of EWHE.

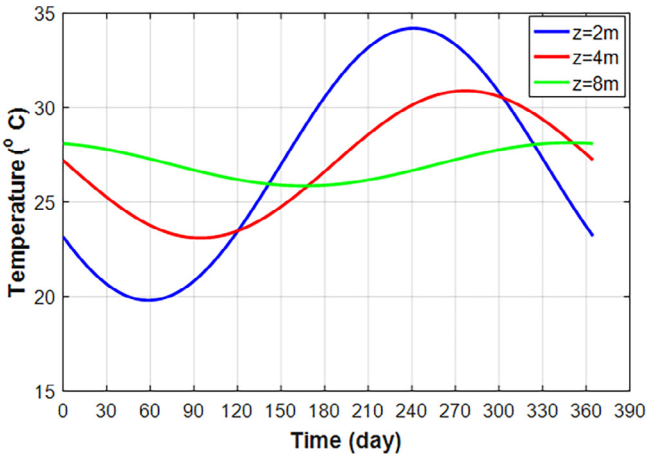

Fig. 12. Yearly soil temperature profiles for different soil depths.

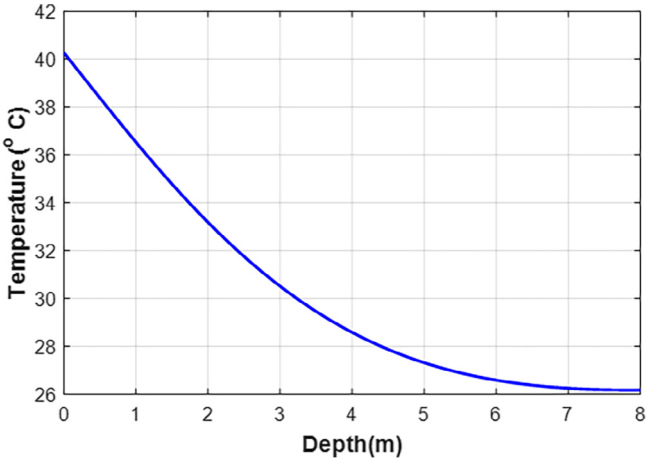

Fig. 13. Soil temperature variation with the soil depth in July.

The average water temperature is given as:

$$Tw_{av} = \frac{T_{w1} + T_{w2} + T_{w3} + T_{w4}}{4} \tag{30}$$

where *SD* and *SE* are standard deviation and standard error respectively.

Fig. 16 shows a comparison between the theoretical results and experimental data for a selected day (August 25, 2017). It's shown that,

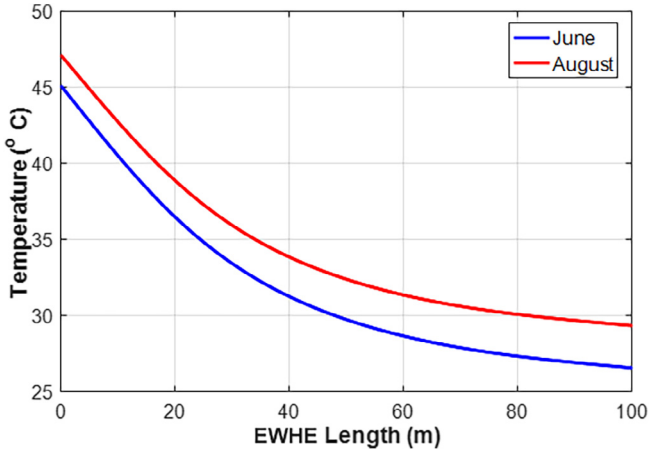

Fig. 14. Outlet water temperature variation with EWHE length for June and August.

Fig. 15. Water temperature reading at 17:00 (water tank of 1 m^3 capacity).

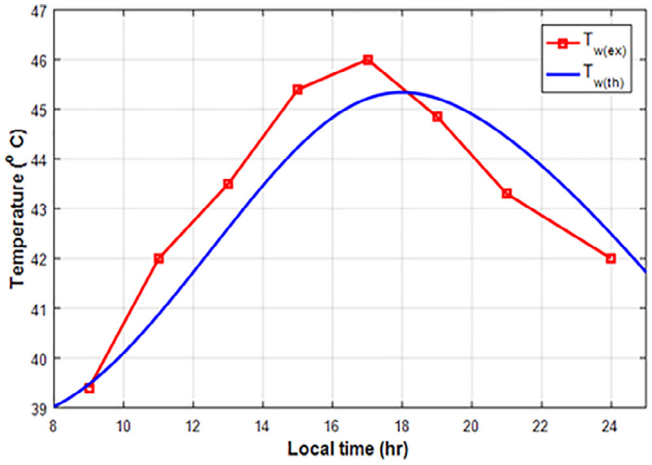

Fig. 16. Comparison of tank water temperature between theoretical and experimental data (25/8/2017).

the experimental temperatures are somewhat higher than that of the theoretical one along the sunshine duration. This may be due to the neglecting of heat transfer from the top and bottom of the storage tank. Error bar of the recorded temperature is shown in Fig. 17 with maximum standard error of 0.64 °C.

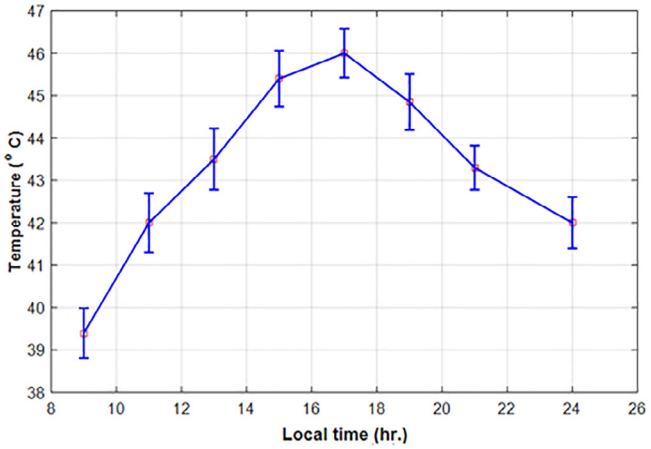

Fig. 17. Error bar of the experimental water temperature recorded on August 25, 2017.

5. Conclusions

1. Earth water heat exchanger is an efficient method to reduce the water to an acceptable level for domestic uses.
2. In south of Iraq maximum water temperature in storage tank is closed to 50 °C during the summer season.
3. The solar intensity and ambient temperature are the main parameters effect of the storage water temperature.
4. The comparison between the theoretical and experimental results shows a good agreement.

Conflict of interest

There is no conflict of interest.

Appendix A. Supplementary data

Supplementary data associated with this article can be found, in the online version, at http://dx.doi.org/10.1016/j.tsep.2018.03.009.

References

[1] N.M. Nahar, K.S. Malhotra, Year round performance of cylindrical solar water heater, Energy Convers. Manage. 24 (4) (1984) 277–280.
[2] S. Saroja, P. Nithiarasu, K.N. Seetharamu, Transient analysis of cylindrical solar water heater, Energy Convers. Manage. 38 (18) (1997) 1833–1840.
[3] F. Al-Ajmi, D.L. Loveday, V.I. Hanby, The cooling potential of earth–air heat exchangers for domestic buildings in a desert climate, Build. Environ. 41 (2006) 235–244.
[4] Faezeh Fazlikhani, Hossein Goudarzi, Ebrahim Solgi, Numerical analysis of the efficiency of earth to air heat exchange systems in cold and hot-arid climates, Energy Convers. Manage. 148 (2017) 78–89.
[5] Sanjeev Jakhar, Manoj S. Soni, Experimental and theoretical analysis of glazed tube-and-sheet photovoltaic/thermal system with earth water heat exchanger cooling, Energy Convers. Manage. 153 (2017) 576–588.
[6] Basharat Jamil, Abid T. Siddiqui, Naiem Akhtar, Estimation of solar radiation and optimum tilt angles for south-facing surfaces in Humid Subtropical Climatic Region of India, Eng. Sci. Technol. Int. J. 19 (2016) 1826–1835.
[7] Latif M. Jiji, Heat Convection, Springer-Verlag, Berlin Heidelberg, 2006 321.
[8] Rajesh Tripathi, G.N. Tiwari, Performance evaluation of a solar still by using the concept of solar fractionation, Desalination 169 (2004) 69–80.
[9] A. Mawire, M. McPherson, Experimental characterization of a thermal energy storage system using temperature and power controlled charging, 2008, 33, 682–693.
[10] Hussein Ali Jabar, Theoretical and experimental study of tubular solar still in Iraq, MSc thesis, Basrah University, Engineering College, 2016.
[11] Fariba Besharat, Ali A. Dehghan, Ahmad R. Faghih, Empirical models for estimating global solar radiation: a review and case study, Renew. Sustain. Energy Rev. 21 (2013) 798–821.
[12] Y. El Mghouchi, A. El Bouardi, Z. Choulli, T. Ajzoul, Models for obtaining the daily direct, diffuse and global solar radiations, Renew. Sustain. Energy Rev. 56 (2016) 87–99.
[13] Y. El Mghouchi, E. Chham, M.S. Krikiz, T. Ajzoul, A. El Bouardi, On the prediction of the daily global solar radiation intensity on south-facing plane surfaces inclined

at varying angles, Energy Convers. Manage. 120 (2016) 397–411.
[14] M.De. Paepe, A. Janssens, Thermo-hydraulic design of earth tube heat exchanger, Energy Build. 35 (2003) 389–397.
[15] Yemna Sarray, Nejib Hidouri, Ali Mchirgui, Ammar Ben Brahim, Study of heat and mass transfer phenomena and entropy rate of humid air inside a passive solar still, Desalination 409 (2017) 80–95.